Critical components for diamond-based quantum coherent devices

Published version:

DOI:10.1088/0953-8984/18/21/S09

A. D. Greentree;P. Olivero;M. Draganski;E. Trajkov;J. R. Rabeau;P. Reichart;B. C. Gibson;S. Rubanov;S. T. Huntington;D. N. Jamieson;S. Prawer. Critical components for diamond-based quantum coherent devices. JOURNAL OF PHYSICS. CONDENSED MATTER. 18 pp: S825-S842.
DOI: 10.1088/0953-8984/18/21/S09

Critical components for diamond-based quantum coherent devices.

Andrew D. Greentree[1,2], Paolo Olivero[2], Martin Draganski[3], Elizabeth Trajkov[4,2], James R. Rabeau[2], Patrick Reichart[2], Brant C. Gibson[4,2], Sergey Rubanov[2], David N. Jamieson[1,2], and Steven Prawer[1,2]

[1] Centre for Quantum Computer Technology
[2] School of Physics, The University of Melbourne, Melbourne, Victoria 3010, Australia.
[3] Applied Physics, RMIT University, GPO Box 2476V, Melbourne. Victoria 3001, Australia.
[4] Quantum Communications Victoria

E-mail: andrew.greentree@ph.unimelb.edu.au

Abstract. The necessary elements for practical devices exploiting non-trivial quantum coherence in diamond materials are summarised, and progress towards their realisation documented. A brief review of future prospects for diamond based is also provided

1. Introduction

The quest to build a quantum computer is one of the most difficult and ambitious technological challenges of the 21st century. It is difficult not just for technical reasons (as the Manhattan and Apollo programs were), but for fundamental scientific reasons as well. Despite the great successes in quantum mechanics, we still have no clear and intuitive understanding of entanglement between large numbers of particles, despite a general understanding that this is the main resource of quantum computers and their point of departure from classical computers [1]. Given this lack of knowledge, there are many in the quantum information community who are suspecting that the pursuit of quantum computers is a naïve exploit. Not because quantum computers are impossible or impractical (there is no evidence as yet to support either assertion: at present they merely appear difficult), but rather because quantum computers represent the tip of the iceberg in terms of surprising and beneficial devices.

Many researchers believe that the technology of the twenty-first century will be *defined* by the exploitation of coherent quantum mechanics, in precisely the same way that incoherent quantum mechanics (tunneling etc.) has defined the semiconductor industry, and hence the technology of the latter half of the twentieth century. Even if some new no-go theorem is shown to preclude a scalable quantum computer: quantum communication [2], quantum control [3, 4, 5], quantum key distribution [6, 7], teleportation [8], entanglement based frequency standards [9], quantum lithography [10] and similar technologies are destined for central roles in science and technology. Such a belief propels one to examine robust systems, where the quantum coherence can be interacted upon, stored, and then extracted into the rest of the world. Diamond offers exactly this possibility.

Diamond has long been recognised as an exceptional material. In many respects it represents an extreme material: it is the hardest material; possesses the largest Young's modulus; the widest optical transparency window; is chemically inert; and can accommodate a wide variety of optically active colour centres (see for example Zaitsev [11]), some which can act as isolated artificial atoms.

Of these colour centres, one in particular, the nitrogen-vacancy (NV) centre has attracted some of the most interest (here we concentrate on the negatively charged version, the NV^- centre, and drop the negative sign except where there is potential ambiguity with the neutral NV^0 centre). This interest is well-justified: following the first detection of single NV centres using confocal microscopy [12], diamonds containing the NV colour centre have shown an enviable list of firsts: first photo-stable single photon source at room temperature [13], first complete demonstration of Quantum Key Distribution (QKD) with pulsed true single photon pulses [14], first observation of single spin measurement and coherent oscillations in a solid at room temperature [15], and first demonstration of tomography of a solid-state (non-superconducting) qubit [16]. Furthermore, such features as multiply-dressed states [17, 18, 19], electromagnetically induced transparency [20, 21], and demonstration of two-qubit coupling [22] have also been reported. With the many successes of NV diamond to date, it is important to ask why such successes are yet to translate into viable quantum devices, and why diamond remains outside the scientific mainstream for both quantum computing and quantum key distribution [23]. Alternatively, one may ask what breakthrough has occurred to force a reappraisal of the potential of diamond for such applications (and others).

To date, we can broadly separate the history of diamond into three important phases. The first is the period from antiquity to the middle of the last century, where diamond was seen as a product to be mined and characterised based on its properties (size, purity, colour etc.). During this time, there was little ability to alter diamond properties, nor to make synthetic diamond of any appreciable quality for optical applications.

With understanding of diamond from a characterisation viewpoint, came the ability to alter the physico-chemical properties of diamond by techniques such as irradiation and annealing: ushering in the second phase of diamond physics - the bulk single crystal phase. In this period the properties of centres, especially the NV centre, were studied in the bulk in samples of high purity and controlled concentration.

The third phase is marked by the ability to explore the dynamics of single centres in diamond for their optical properties. In the main, this work utilised nanodiamond formed from exploded single crystal diamond. This means that the grain sizes are small, and surface effects large, and often highly variable from site to site. Furthermore the potential to scale up such devices is minimal. An important alternative is the growth of Chemical Vapour Deposition (CVD) diamond films on pre-existing optical structures (e.g. optical fibres [24]), however these devices are still insufficient for quantum computing applications, or for protocols requiring more than one identical atom/photon. Issues of reproducibility, scalability and optical transparency all need to be overcome before the potential of diamond can be fully realized.

The fourth phase is the era we are entering at present. This fourth phase is defined by placing single, optically active centres at defined locations within optically important structures carved out of single crystal diamond. Examples of the kinds of structures of particular interest are waveguides and photonic bandgap cavities. This has not been possible until the mechanism for defining such structures existed, and the features of diamond (especially its hardness, inertness, and to a lesser extent its transparency) which make it so desirable have also prevented such fabrication. The lift-off technique [25, 26], combined with single-ion implantation [27, 28] are the enabling technologies which usher this new era of diamond photonics. Associated is the technology required to selectively address individual centres, and to controllably mediate interactions between individual centres. Lastly are methods to readout single centres, or to otherwise outcouple useful signatures of the quantum coherence, for example transform limited single photons, or entangled photon pairs.

This review explores the emergence of the fourth-phase of diamond quantum research. We will briefly cover some of the proposed applications for quantum coherent devices in diamond, especially architectures for quantum computers, but this is not the main focus of this work. Rather this review seeks to identify the advantages and challenges faced by diamond in constructing practical devices.

The solution to the placement problem is associated with another problem, ubiquitous to quantum systems of all types, but especially those in the solid state, namely particle distinguishability. Scalability of a quantum computer, requires that the qubits (quantum bits, the equivalent of bits in classical computers) be distinguishable in some degree of freedom that is, in some sense, unbounded. The obvious degree of freedom is space, i.e. qubits are distinguished by their *position* within a quantum device. Concomitant with this, is the need for their other parameters (e.g. transition energy, nearest neighbour coupling, and interactions with local control gates) to be as similar as possible. Such competing requirements immediately rule out many proposed implementations (e.g. homogeneous atomic groupings with inhomogeneously broadened spectral lines) as being ultimately unscalable (although they may be useful in short-term applications). Liquid state NMR [29] is a prime example of an unscalable architecture which has nonetheless proved exceedingly useful in advancing the field (see for example Ref. [30]). Mentioned above was that the spatial problem of creating atoms at well-defined positions has been addressed in NV diamond [28], although there are outstanding issues regarding yield and placement accuracy, associated with that is the technology to connect the different centres which will be discussed below. However, the spectral inhomogeneity of NV centres would give rise to intolerable limitations on scalability without a reliable mechanism to tune the atoms to the same resonance. A method based on Stark shifting has long been proposed for this, and we will discuss this with regards to single centre work.

This review is divided, into three main sections. The first is a brief summary of some of the proposed implementations for diamond based quantum computing, to highlight commonalities, rather than to decide the optimal implementation: it is fair to say that the “ideal” architecture is not yet known. We will then discuss a method for fabricating microstructures within single-crystal diamond. Finally we address methods of creating indiviual NV centres in spatially defined locations.

2. Quantum computing architectures

There are (at least) five alternative proposals for entanglement generation, and quantum computing in NV diamond systems, of which three specifically use some properties of NV diamond, and two where NV diamond is merely a convenient system for their realisation. Although it is not the purpose of this article to provide a comprehensive review of diamond-based quantum computing schemes, we will outline some of the proposals, so as to highlight some of the components necessary for each. Note that there are also many other schemes (e.g. cavity QED [31, 32], optically-coupled quantum dot [33] and linear optical [34] schemes) that could be easily converted to NV diamond implementations. As will be seen, although many of the details are quite different, the actual structures required are very similar. Because of the central role played by Stark shifting in most NV based quantum computing schemes as a means for tuning centres into and out of resonance with each and external pumps, we will briefly discuss this issue separately. In addition to quantum computing, NV has been specifically suggested for other quantum device applications, including quantum repeaters [35] and as a quantum Q-switch [36]. Applications to QKD have been noted above.

2.1. Stark tuning of NV centres

The linear Stark shift is the perturbation of the energy levels of an electric dipole, when placed in an external electric field. It is written as

$$E_s = \overrightarrow{p} \cdot \overrightarrow{\mathcal{E}} \tag{1}$$

where $\overrightarrow{p}$ is the electric dipole moment, and $\overrightarrow{\mathcal{E}}$ is the external applied electric field. The idea of using the Stark effect to shift transitions into resonance was introduced by Brewer and Shoemaker [37] as a new spectroscopic technique in their studies of molecules. Apart from finding application in a wide range of fields, it has also become a nearly ubiquitous part of NV based quantum computing, as it represents one mechanism for overcoming the inhomogeneous linewidth of NV diamond.

To recap the problem: the lifetime of the ^{3}E state (the first optically excited manifold) of NV diamond is around $T_1 = 12$ ns, depending on the exact sample and conditions [38], implying a linewidth of $\omega_h = 2\pi/T_1 = 50 \times 2\pi$ MHz. However in ensembles, the inhomogeneous linewidth (i.e. the linewidth arising from local perturbations to the optical transition frequency) is generally accepted to be $750 \times 2\pi$ GHz. Assuming that a randomly chosen centre will have a frequency somewhere within this distribution implies that all schemes based on optical coupling require some degree of tuning of the transitions so as to be either mutually resonant or significantly off-resonant with neighbouring centres, or some external control field. The Stark shift offers a potential solution.

To calculate the expected Stark shift in NV diamond, we note that the dipole moment of the NV centre is simply given by the charge (one electronic charge, q_e) separated by the atomic spacing of diamond $a = 0.15$ nm, and so the frequency shift felt by a centre aligned parallel to a uniform electric field can be easily determined by rearranging (1), i.e.

$$\omega_S = \frac{q_e a}{\hbar}\mathcal{E} = 2.3 \times 10^5 \mathcal{E}. \tag{2}$$

The Stark effect has been observed qualitatively in NV diamond several times previously [39, 40], although the canonical quantitative reference is from Redman *et al* [41]. In Ref. [41] a homogeneous sample of NV centres was prepared via persistent holeburning, then a uniform electric field was applied, and its effect on the hole monitored. Although the centres in the spectral hole were homogeneous with respect to the transition frequency, they were not homogeneous with respect to the applied field, and so although one would expect the homogeneous line to split

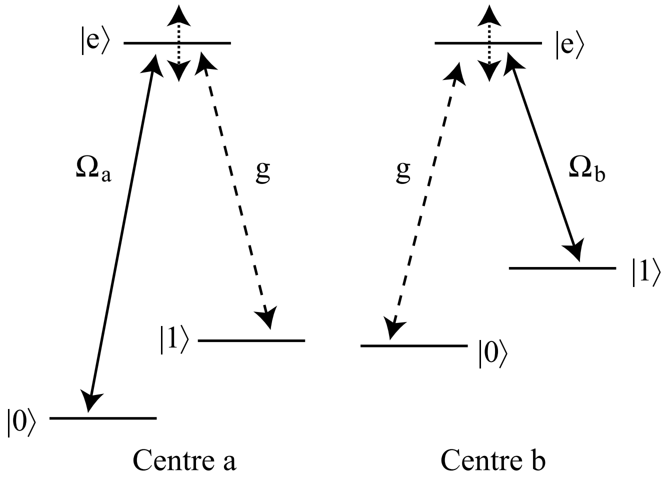

Figure 1. Scheme for resonant dipole-dipole interactions between two three level atoms. In each atom, the two-photon transition can be mediated conditionally on the state of the other atom. The atom-atom coupling strength is either determined by the proximity of the atoms to each other, or can be long-range if mediated by a cavity photon.

into eight different lines, in fact only a broadening of the line was observed. From this broadening it is possible to estimate the largest shift (corresponding to centres aligned parallel or anti-parallel with the field) as being

$$\frac{\omega_s}{\mathcal{E}} \sim 5 \times 10^4 \times 2\pi \text{ HzmV}^{-1}, \tag{3}$$

which is in passable agreement with the simple prediction above, at least until more precise single centre data is available.

Alternatively, we may calculate the electric field required to shift a centre by one inhomogeneous linewidth ($\sim$ 750 $\times$ 2π GHz), which is of order 10^7 Vm^{-1}, or 0.1 MVcm^{-1}. This field is significantly less than the field required to cause breakdown in single crystal diamond of 10 MVcm^{-1}, which is, incidentally, the largest of any known material [42].

2.2. Resonant dipole-dipole coupling

Two-qubit interactions have been proposed by using resonant dipole-dipole coupling to controllably entangle NV centres [43, 44]. The coupling exploits the Stark shift and the three-level nature of the NV centres to achieve Raman transitions that are conditional on the state of nearby centres. The idea can be understood with respect to Fig. 1.

Consider two atoms, a and b, in the Λ configuration, where the qubit states are the ground states, $|0\rangle$ and $|1\rangle$, and these are two-photon coupled via the excited state $|e\rangle$. Two lasers are applied, one resonant (or quasi-resonant) with the $|0\rangle_a - |e\rangle_a$ transition with Rabi frequency Ω_a, and the $|1\rangle - |e\rangle$ transition coupled by a field with Rabi frequency Ω_b. In this arrangement, note that the frequencies of the $|e\rangle_a - |1\rangle_a$ and $|e\rangle_b - |0\rangle_b$ transitions are equal, so there will be an effective coupling between these transitions via virtual photon exchange if the atoms are in close proximity, or alternatively, if the atoms communicate via a shared cavity mode that is initially unoccupied. This extra coupling, g is state dependent and allows non-trivial phase shifts, and hence conditional quantum logic to be performed, for example via conditional Raman adiabatic passage [43] or state information transfer between qubits via the shared channel [44]. Qubit selectivity is achieved by Stark tuning two atoms so that the required coupling schemes and resonances are achieved.

Ultimately scalability in this scheme will be limited by issues such as the drop off of the dipole-dipole coupling with distance, and ratio of homogeneous to inhomogeneous linewidth, or in the case of cavity mediated interactions, by the limited number of parallel operations that can be carried out (multiple occupation of the cavity will be problematic). Nevertheless, both schemes appear possible for of order 100 qubits, enough for convincing demonstrations. Although 100 qubits is not enough for non-trivial quantum computing when error correction is required.

2.3. Weak nonlinearities

Historically, one of the earliest suggested implementations of a quantum gate was to use a material exhibiting a large, lossless Kerr-type nonlinearity in the path of an interferometer. Such an approach was outlined by Milburn [45], and has been expanded upon many times (see e.g. [46, 47]).

Conceptually, the approach to quantum computing via nonlinear optics is very simple. An interferometer is set up as shown in Fig. 2(a), where pairs of rails describe a qubit defined by a single photon in some superposition of each interferometer arm: dual rail notation. Essentially the top pair of arms is a Mach-Zehnder interferometer with a Kerr-type nonlinear medium in one arm. It is balanced so that if 0 or 1 photons pass through the nonlinear medium, the target photon leaves in the same state as it enters the interferometer. However, if the control photon in the state $|1\rangle_C$, then there is a phase shift such that the state of the target is reversed, realising a Controlled-NOT, CNOT, gate.

The essential problem with all such schemes, however, has been the lack of a suitable medium that can generate the required phase shift ($\pi/2$) at the single photon level, without absorbing either control or target photon. Although there have been many suggestions for electromagnetically induced transparency (EIT) [48] and cavity-QED processes to generate the required nonlinearity [31], a somewhat surprising alternative has recently been proposed.

It was recently realised [49] that efficient photon counting Quantum Non-Demolition (QND) detectors could be realised in a material exhibiting a weak, lossless nonlinearity, precisely the nonlinearity observed in EIT systems, without the requirement for a $\pi/2$ conditional phase shift. The device functions similarly to high-precision dark fringe interferometry. An interferometer is set up for a strong coupling field, aligned so that one output port sees a dark fringe, see Fig. 2(b). One arm of the interferometer has a cross-Kerr nonlinear medium, and the probe (to be detected) and one of the states of the qubit field pass through this medium. The weak nonlinearity induces a slight phase shift, θ on the probe field, dependant on the presence or absence of photons in the qubit arm. This phase shift is detected by performing a homodyne measurement of the output light. Of course this phase shift will be extremely small, however the signal will be proportional to both the phase shift and coupling intensity, effectively enhancing the weak nonlinearity.

The QND detector can be used as a primitive for more complex detectors, e.g.

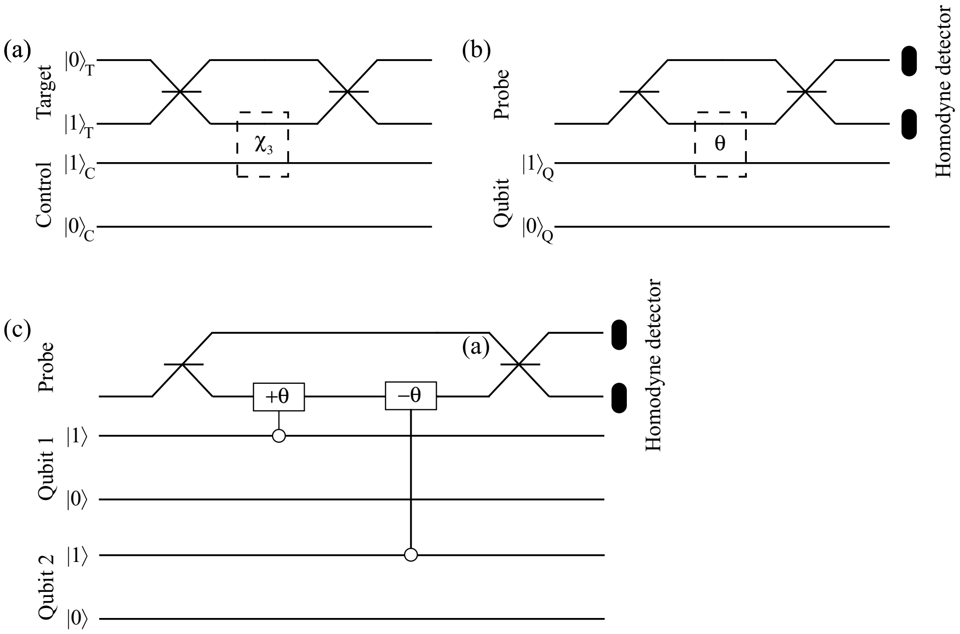

Figure 2. (a) Canonical scheme for CNOT operation with an ideal, lossless nonlinear medium (dotted box marked $\pi/2$) capable of providing a $\pi/2$ phase shift to the target, if the control photon is in the $|1\rangle$ state. (b) QND detector based on the weak nonlinearity scheme. A phase shift of $\theta \ll \pi/2$ is induced in the probe field by the presence or absence of a photon in the state $|1\rangle$, and this phase shift is detected by performing homodyne detection on the probe. (c) Parity gate exploiting the QND detector as a primitive. In this case the first interaction is a conditional phase shift of θ on the first qubit, and $-\theta$ from the second qubit. More complex schemes are possible, including CNOT gates, and hence universal quantum computation.

a parity detector for a two-qubit system [Fig. 2(c)]. Here, the probe field acts as a bus, and with appropriate choice of applied nonlinear phases, effects coupling between different probe fields [50], and classical feedforward can be used to be project the qubits into the required states. Suitable choices of coupling and geometry permit a full Bell state analyser and near deterministic CNOT gate [51].

Although this approach can be applied to a large number of different implementations [52], NV diamond has a privileged place amongst optical/solid state implementations. The reason is that in order to amplify the (admittedly very small) lossless nonlinearities, very intense probe fields will need to be applied, which may tax materials properties such as melting point (for example in silica fibres). The fact that diamond has both the highest thermal conductivity and heat resistance makes therefore makes it the ideal choice for such implementations [53].

2.4. Repeat until success quantum computing

In principle, single qubit operations in NV diamond are relatively easy in either ensemble [54, 55, 56] or single centre [15] implementations. Despite measurements of NV-^{13}C [22] and NV-N coupling [57], as of writing, we are unaware of any unambiguous demonstrations of NV-NV coupling. Although there is no reason to suggest that this will not be possible, there are interesting alternative schemes, where qubit-qubit coupling can be achieved *without* direct two-qubit interactions, using instead measurement induced interactions.

The idea behind measurement-induced schemes is that individual qubits can be housed in separate cavities, and emitted photons from the cavities can be mixed on beamsplitters in a fashion so as to erase which-path information. In this way, conditional detection at beamsplitters projects the qubits onto entangled subspaces, with the exact entanglement generated being conditional on the measurement outcome. Two such schemes were introduced almost simultaneously, namely the 'Repeat-Until-Success' scheme of Lim, Beige and Kwek [58] and the 'Double-Heralded' scheme of Barrett and Kok [59]. One of the very attractive features of both schemes is that if the protocol fails, then it can be repeated without any additional error to the overall quantum operation. The schemes are therefore highly suitable to the non-deterministic generation of entangled states, and indeed, graph-state schemes along these lines have been proposed [60, 61].

Related to these non-deterministic, but heralded, schemes is a deterministic protocol that exploits the very powerful technique of operator measurements [62]. In these schemes a joint measurement of some two-qubit operator is performed which is chosen to project the isolated matter qubits into an eigenstate which corresponds to an entangled subspace. Because the matter qubits are projected into an eigenstate, additional applications of the operator measurement simply project the qubits into the same eigenstate, hence the scheme is highly robust to loss of the detected photon. A scheme to realise such operator measurements in a highly general fashion (using the stabiliser formalism) has been presented [63], although that work was highly general and not specifically NV based.

2.5. Brokered graph state

Cluster states were originally proposed as an alternative paradigm for quantum computing in two-dimensional Ising lattices [64], however it is arguably true that it is in the field of linear optics quantum computing that their true utility has been identified [65, 66, 67]. The approach in [66] is especially interesting. In this scheme a mechanism for fusing cluster states is introduced that succeeds with 50% fidelity (shrinking the clusters with failure), so that appropriate choice of starting states is necessary for scalability (i.e. so that there is a net probability of increasing the size of the cluster state). This elegant proposal has been shown to dramatically decrease the overheads in terms of single photons to realize non-trivial quantum logic, over both the original KLM [34] and Nielsen [65] schemes.

Although it is obvious and natural to suggest that one-way quantum computing might be performed in NV diamond, it is far less easy to find a non-trivial implementation. A rather striking scheme has recently been proposed which is far from trivial, and uses NV centres (or systems with similar energy level schemes) in an essential fashion: Brokered Graph State Quantum Computing [68]. In this scheme entanglement between the 'brokers' is attempted (using, for example, the schemes described in 2.4) and when succesful (indicating by appropriate heralding) the entanglement is transferred to the clients. In the NV scheme, it is envisaged that the relatively easy to control electronic spins would be the brokers, and the well-isolated nuclear spins would be the clients. Because the electron and nuclear spins can be effectively isolated unless interactions are desired, failure of the brokering does nothing to damage the existing client state entanglement.

3. Fabricating micro-structures in single crystal diamond

The very properties that make diamond so attractive as a material (especially hardness, chemical inertness) make the micromachining of diamond extremely challenging [69, 70, 80]. Most existing techniques are based on the use of Chemical Vapor Deposition (CVD) of polycrystalline films combined with selective ablation or replication processes that employ masking and moulding. Recently, sophisticated three-dimensional nano-structures were fabricated in nanocrystalline diamond [73, 74]. Although such structures have promising applications in micro-electromechanical system (MEMS) technology, defect-free single-crystal diamond is required as the substrate for integrated quantum-optics devices. This requirement arises from the necessity for identical environments for each qubit. Combined with this is the fact that the optical quality of most CVD films is poor compared to that of Silica or Silicon.

A new method for the fabrication of free standing micro-structures in bulk single-crystal diamond was recently demonstrated [26]. The method is inspired by the "diamond lift-off" technique [25, 75], and takes advantage of the fact that, by means of ion implantation, it is possible to induce a phase transformation from diamond to a selectively etchable phase (the sacrificial layer). Here we briefly summarize the micro-fabrication process and report on the creation of a waveguide microstructure.

The sacrificial layer is created by the transformation induced by MeV ions which deposit most of their energy at the end of range, creating a spatially well-defined disordered region (see schematics in Fig. 3(a) and optical microscopy image in Fig. 3). The results demonstrated [26] employed 2 MeV He ions in synthetic High Pressure High Temperature (HPHT) diamond crystals, which created a 500 nm thick buried sacrificial layer located 3.5 μm below the surface. These conditions are by no-means restrictive, and control of the energy, fluence, and implant species will all determine where most of the lattice transformation occurs, and this has been studied in more depth previously [76, 77, 78]. Hence it is possible to control the vertical location of the sacrificial layer to sub-micron resolution [79].

To facilitate etching, the buried sacrificial layer must be exposed to the etchants, and hence some kind of milling must be employed. Laser ablation is one method [80, 72], but patterned milling with a Focused Ion Beam (FIB) is our preferred method as the spatial resolution of the FIB is in principle much finer, allowing nanometer scale features to be drawn [81, 82] as shown schematically in Fig. 3(b) with the relevant SEM image in Fig. 3(f).

Thermal annealing is employed to convert the sacrificial layer to an etchable material with respect to the chemically inert diamond phase, while partially recovering the pristine diamond structure in volumes exposed to lower energy deposition. Wet chemical etching in boiling acid solution removes the exposed sacrificial layer, while leaving the diamond structure intact. This process is depicted schematically in Fig. 3(c), while Fig. 3(g) shows optical microscopy images of the sample at different stages of the etching process. Other efficient etching strategies, such as annealing in oxygen atmosphere [25, 75] or electrochemical etching [83], can also be employed. After selective etching, unconnected surface diamond layers lift off, leaving behind the desired patterned structure, which may include undercut regions, as shown in Fig. 3(d), together with the SEM image of the final structure in Fig 3(h). A final

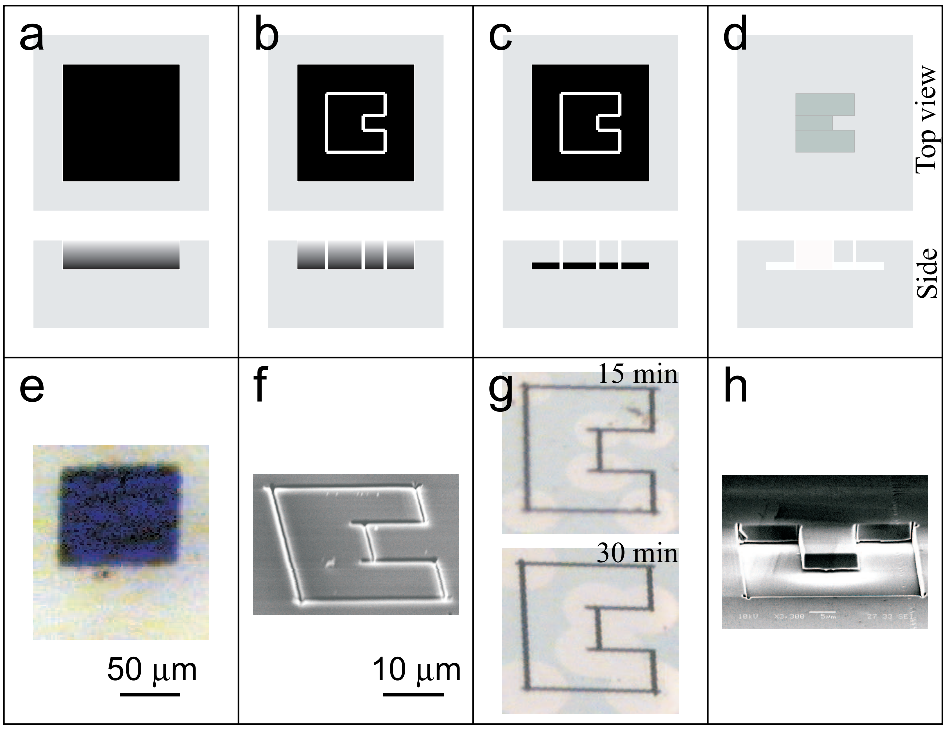

Figure 3. Schematics illustrating the FIB-assisted lift-off process (a-d). Single crystal diamonds are implanted with a 2 MeV He ion microbeam in 100×100 μm squares (a); then patterned with a FIB to expose in defined regions the buried sacrificial layer (b); thermal annealing turns the highly damaged regions into a selectively etchable material (c); upon etching, regions unconnected to the undamaged diamond lift-off, leaving undercut microstructures in the diamond crystal (d). Images showing progress through the procedure (e-g). (e) Optical image of the MeV ion implanted region in diamond crystal, which is rendered opaque by the implantation. (f) SEM image of the FIB patterned area. (g) Optical images of the patterned region during progressive etching steps (after 15 and 30 min, respectively). (g) SEM image of the final (free-standing) structure after lift-off of the unconnected regions.

thermal annealing step is also required to recover the pristine diamond structure from residual damage induced from both ion implantation and ion patterning.

A test structure comprising a free standing bridge waveguide in single crystal diamond is shown in the SEM image in Fig. 4. With the same procedure, a range of three-dimensional structures (cantilevers, cavities, beamsplitters, etc) can be created in bulk diamond with sub-micrometer spatial resolution, and these are currently being investigated. The remarkable smoothness of the bottom surfaces after lift-off is due to the abrupt damage threshold for phase transformation upon annealing that leads to a sharp interface between diamond and the sacrificial layer, while the roughness of the lateral surfaces is defined by the accuracy of the FIB milling process, which can be significantly improved with vapor-assisted methods [84]. A more detailed description of the micromachining technique, together with an extensive characterization of the material properties of the structures during the fabrication process, can be found

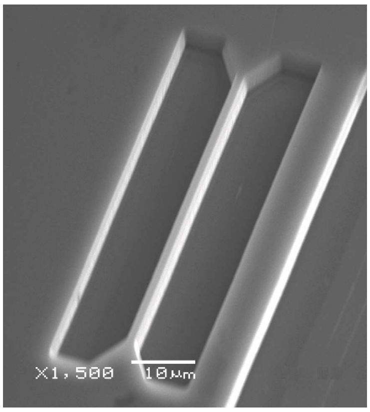

Figure 4. SEM image of a waveguide structure created in single-crystal diamond with the FIB-assisted lift-off technique; the structure has a cross section of 3.5×2 μm thick, while the 500 nm undercut is visible.

elsewhere [85].

4. Methods of implanting optically active centres in diamond

Ion implantation offers the possibility for the direct placement of NV centres in diamond with nanometre scale precision using technologies developed for the placement of single P donors in silicon [27]. However unlike the case of silicon for diamond, two alternative routes are available for the creation of NV centers.

The first method for NV creation involves implantation to create vacancies in nitrogen-rich type Ib diamond. Annealing above 600°C causes the vacancies to migrate to the intrinsic substitutional nitrogen sites to form NV^0 and NV^- centers. Exposure of diamond containing nitrogen to almost any kind of irradiation, followed by annealing above 550°C leads to formation of NV centres [86, 11], and specifically implantation of neutrons [87], protons, electrons, gallium [88], helium, carbon and other ions have all been employed for NV formation with this method. With this technique, NVs are formed from the nitrogen so this method is best suited to creating ensembles or small ensembles of centres.

The second approach to NV formation involves the direct implantation of nitrogen ions into type IIa diamond containing low concentrations of nitrogen, followed by thermal annealing. This approach promises greater control of the absolute number of centres, down to the single centre level, which is necessary for the fabrication of arrays of single NV centers. Importantly, since one of the main causes of decoherence in NV centres is spin flips due to the presence of excess nitrogen spins (and to a lesser extent, background ^{13}C, and we note that pure ^{12}C is available for ultra-heat sinking applications) [55], the use of high purity crystals is essential to increase decoherence times.

Sourcing diamond with the prerequisite low nitrogen background is challenging, a fact that has impeded research into NV for quantum information applications. An important parameter for the scalability of fabricating arrays of NV centres by ion implantation is the probability that a single implanted nitrogen will result in an observable and usable NV centre.

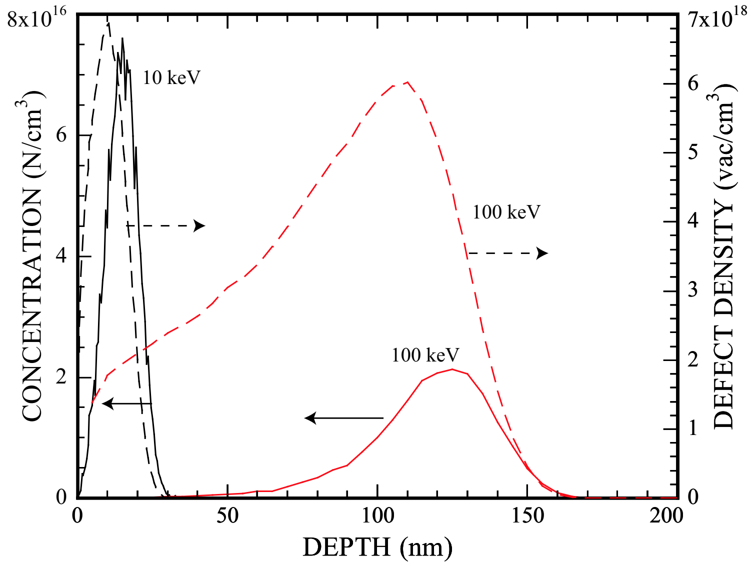

Figure 5. SRIm simulation of 10 and 100 keV N ions into diamond. A fluence of 1×10^{12} N/cm^2 has been used in the simulations. The solid lines (scale on the left hand axis is the N concentration due to the implanted ions. The dotted lines (scale to the right hand axis) show the corresponding vacancy concentration induced by the implanted N. Note that the vacancy concentration is about two orders of magnitude higher than the concentration of implanted N. Therefore unless ultrapure diamond is used, the probability that a native N will be converted to NV will exceed the probability that the implanted N will result in a NV centre.

Nitrogen has been implanted into diamond to create NV centres previously [89, 28]. Perhaps surprisingly, however, the measurement of the conversion efficiency of *implanted* nitrogen to NV is difficult and not resolved in the previous works. Figure 5 shows the results of a SRIM [90] simulation of the implantation of 10 and 100 keV N atoms into diamond. Note that for each implanted N, more than 80 and 300 vacancies are produced for 10 and 100 keV implantations respectively. Consequently there is a high probability that any pre-existing nitrogen near or within the track of the implanted ion will be in close proximity to a vacancy, and hence be converted into an NV centre upon annealing. Therefore if the direct N implantation approach is adopted, a background nitrogen concentration of less than approximately 7 and 0.05 ppm for 10 and 100 keV implants respectively is required to avoid the native N swamping any implanted N. We understand this, as the higher energy implants affect a much larger volume of material; so to ensure that on average there are very few native N in the affected volume a lower background N concentration is required. Hence measuring the probability that an implanted N will result in a single NV being created is complicated. As explained below, this problem can be addressed by the implantation of ^{15}N and the detection of ^{15}NV which, via the hyperfine splitting, can be distinguished from ^{14}NV centres [91]. We now discuss each method in turn.

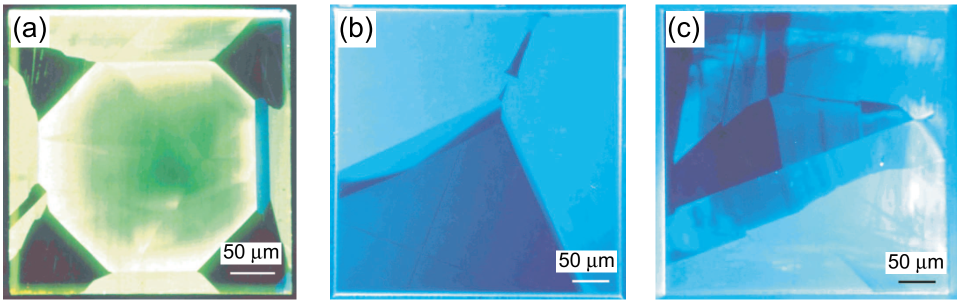

Figure 6. Cathodoluminescence maps of type Ib HPHT [100] crystal (a) and type IIA HPHT diamonds sourced from Sumitomo Diamond Corporation. (b) [100] and (c) [111] crystals; although all three samples are mono-crystalline, growth sectors are clearly visible in all crystals. The sectors exhibit different luminescence properties reflecting their varying impurity and defect compositions. Each individual diamond displays a unique sector signature which must be taken into account when considering the effect of implantation.

4.1. Direct implantation of vacancies

As stated above, the implantation of even low fluences of inert ions can result in the formation of NV centres due to the 'activation' of nitrogen in the sample. In this case it is clear that the resultant NV concentration will depend primarily on the pre-existing N concentration within the track of the implanted ion. In this regard it is important to note that N is often not uniformly distributed throughout a sample. Figure 6(a) is a flood Cathodoluminescence (CL) map of a high-pressure/high temperature Sumitomo type Ib diamond. Strong growth sectoring is clearly evident and is thought to arise arise from the fact that the diamond crystals grow out from a single seed. The growth sectors have been imaged in CVD single crystals by TEM [92]. Raman spectroscopy [93] has shown that the different growth sectors (mainly 100 and 111) also contain different levels of defects. The probability of incorporation of impurities and defects is, in general, higher for the 111 than 100 growth sectors. The results of ion irradiation implantation will therefore depend on which sector is implanted. Because the sectoring is often not evident under an optical microscope, experimentalists are often unaware of the spatial inhomogeneity of the nitrogen concentration. Moreover, there is often inhomogeneity in the incorporation of other impurities (e.g. Ni or vacancies) as well as strain fields set up by the sector boundaries. This may result in lack of reproducibility between reported results, and needs to be taken into account in all measurements on such sectored samples. Strong sectoring is also apparent in Sumitomo diamonds which have a low native concentration of N [Figure 6(b) and (c)].

To explore of the use of N implantation into type 1b samples, squares of area 50×50 μm^2 were irradiated with 30 keV Ga ions ($R_p \pm \Delta R_p = 15 \pm 3$ nm, where R_p is the projected range) using a focused ion beam, over a wide range of fluences from 1×10^9 to 1×10^{18} ions/cm^2. The sample employed was a type Ib HPHT diamond and care was taken to perform all the irradiations were within the same sector. The sample was isochronally annealed from 200°C to 1000°C for 1 hour in an Argon atmosphere.

Figure 7 shows the intensity of the NV^0 and NV$^-$ Zero Phonon Line (ZPL) normalized to the intensity of the first order bulk Raman line as a function of ion fluence for a sample annealed at 800°C. From measurements of the normalized

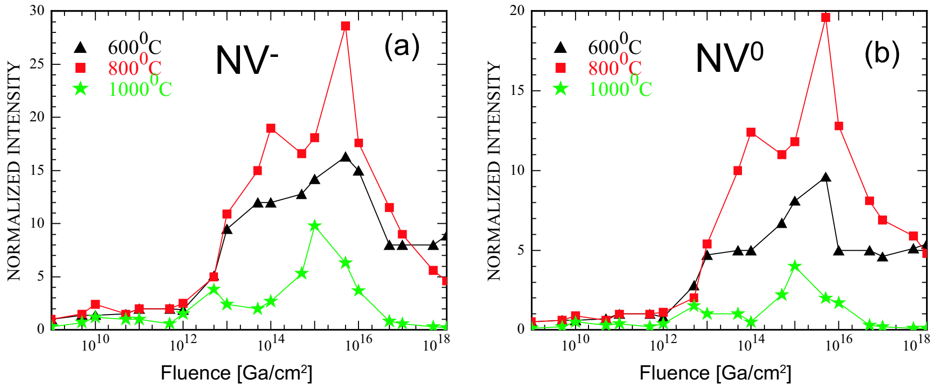

Figure 7. The intensity of the NV^0 (575 nm) and NV^- (637 nm) ZPL normalized to the intensity of the first order Raman mode (at 1332 cm^{-1}) as a function of Ga ion dose. The Ga ion energy was 30 keV. Data for post-implantation annealing at 600, 800 and 1000°C is shown. The PL was excited by 514 nm excitation and the spectra collected at 77 K.

intensity versus ion fluence and annealing temperature, it may be inferred that for the most intense NV emission, the optimal annealing temperature is about 800°C and the optimal fluence about 5×10^{15} Ga/cm^2. This fluence corresponds to about one monolayer, i.e. to complete coverage by the Ga beam of the entire surface. Since each Ga impact creates more than 250 vacancies per incident ion, it is not surprising the saturation of NV production occurs when, on average, the entire irradiated area has been impacted by at least one Ga ion. Note, however that the optimal conditions for maximum intensity do not necessarily correspond to optimal quantum optical properties of the centres thus produced. For example, the ZPL FWHM of the centres at high Ga fluences is much larger than those formed at low fluences.

By performing ion implantation through a micron scale mask, the damage will be localised to the regions exposed to the ion beam, and hence arrays of NV centres will be produced. A fluorescence image showing an NV array generated by this method is shown in figure 8. The fluorescence was imaged using a confocal microscope. Although the bright spots in figure 8 are clusters, rather than single N-V centers, the result proves that such arrays can be created quickly and easily in diamond. Scaling this to single N-V can be accomplished by irradiating through nanoscale, rather than micron scale masks. For example, if the irradiation is performed through a 20 nm aperture, and assuming a background N concentration of 1 part per million, on average about one NV centre will be created per aperture. Following the implantation, transparent conducting electrodes (eg ZnO, ITO) can be deposited through the masks to create electrical contacts registered to the single NV centers. Such registration is necessary for Stark shift tuning of individual NV centres (see subsection 2.1).

It should be recognized that this technique does not allow for precise control of the number of centres in a given spot, and will produce, at best, pseudo-ordered arrays in which locations on the array will have a (small) number of NV centers controlled by Poissonian statistics. Nevertheless, it does allow rapid testing of many key parameters, such as, for example, the registering of transparent electrodes to small clusters, and the

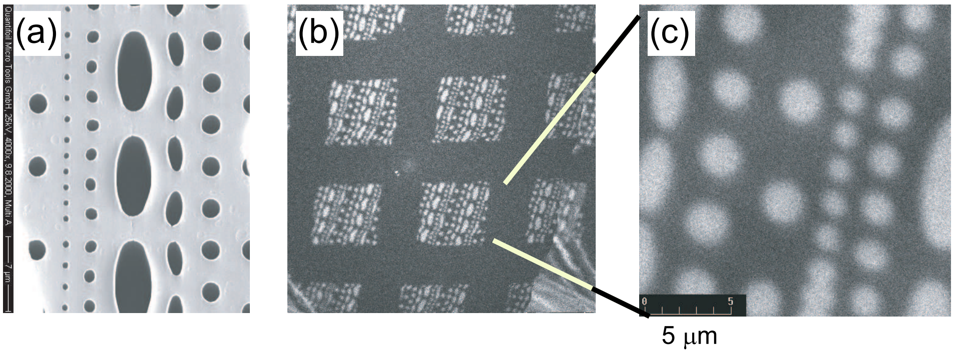

Figure 8. Patterning of NV centres in type Ib diamond via implantation through a mask. (a) shows the quantifoil carbon grid used to mask the sample during ion implantation. The grid was coated with Au to increase the stopping power. Confocal luminescence imaging (b) and (c) shows that the mask pattern is faithfully transferred to the sample.

refinement of the optical detection techniques. Given the relative ease of identifying NV centres, post-selection on centres with the required characteristics may be a viable option for many applications.

4.2. Direct implantation of single nitrogen ions

In principle, deterministic control of the number of NV centres in a given region can be obtained by the implantation of single nitrogen atoms or molecular dimers directly into high quality diamond with little or no N background. Basic concerns have been raised that this technique will result in too much residual damage to allow for the reliable fabrication of a single qubit. However, as a demonstration of the effectiveness of the scheme, N_2 has been implanted at extremely low fluences into very low nitrogen content diamond. Figure 9 shows a plot of the ZPL for various fluences of 14 keV N with the inset showing the FWHM as a function of N concentration. In this case the maximum possible NV concentration corresponds to the implanted N concentration. For ensemble measurements it would appear that NV concentrations as low as 1×10^{18} NV/cm^3 are quite easily resolved.

For the fabrication of qubits via direct N implantation, it is desirable that each implanted N creates a single NV, and that there is no excess N. Hence the probability of forming an NV center under these conditions must be known. This is difficult because it is not obvious how to distinguish between native and implanted NVs in photoluminescence. However, by implanting single ^{15}N ions instead of ^{14}N, a mechanism is available to measure the yield [91]. ^{15}N is a spin 1/2 nucleus and therefore, ^{15}NV has a different hyperfine spectrum from ^{14}NV (which is a spin 1 nucleus). Because the natural abundance of ^{15}N is 0.37%, the observation of ^{15}NV at fractions greater than this provides a clear spectral signature of their origin. Initial measurements [91] in unoptimized conditions, indicate that approximately 2.5% of implanted ions gave rise to optically observable NV centres: all of those measured being ^{15}NV. The experimental conditions for that work had not been optimized, and we expect further developments (e.g. cold implantation [94], or optimal implant energies [28]) to improve yields further.

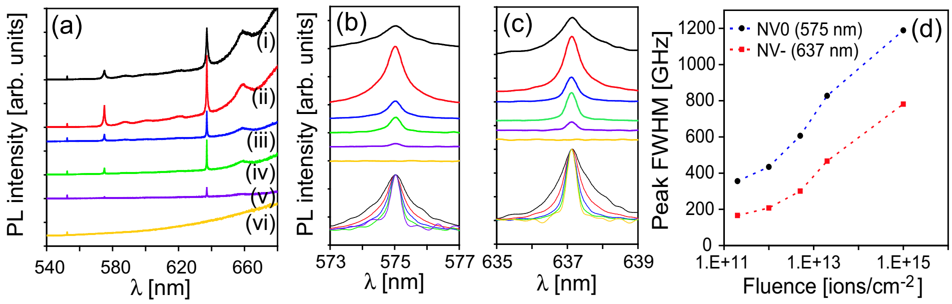

Figure 9. (a) Photoluminescence spectra from regions implanted at varying ion fluences into high quality type IIa diamond crystal. The fluences were: (i) 1×10^{15} N/cm2, (ii) 2×10^{13} N/cm^2; (iii) 5×10^{13} N/cm^2; (iv) 1×10^{12} N/cm^2; (v) 2×10^{11} N/cm^2; (vi) 2×10^{10} N/cm^2. All spectra are normalized to the intensity of the first order diamond Raman line and displaced vertically for clarity. (b) and (c) show zoom spectra of NV^0 and NV$^-$ zero phonon lines, respectively; in the bottom part of the graph, the spectra are overlayed to emphasize the monotonic sharpening of the peaks with decreasing ion fluences. (d) reports the width of the NV^0 and NV$^-$ zero phonon lines in frequency units, as a function of the ion fluences.

5. Conclusions

The motivation for the use of diamond in quantum computing lies primarily in the availability of an 'optical handle' i.e. a reliable and robust optical method for single spin read out and qubit control. There is no doubt that the NV centre in diamond is the best present candidate for a solid state qubit operating at room temperature. The optical handle gives other possibilities as well, however, as it allows for the generation of entangled photons, increasing the utility of 'stepping-stone' devices, en route to full-blown quantum computing.

However, to translate this potential into usable devices requires the development of a nanofabrication toolkit for diamond. Specifically, the key elements needed to engineer qubits in diamond require (i) sourcing and characterizing materials of sufficient purity, (ii) the ability to pattern individual NV centers in diamond and register them to electrical gates, (iii) the ability to tune the optical output of a single NV using the Stark shift, (iv) the ability to fabricate waveguides input-output mirrors in single crystal diamond and (v) establishing the capability for coupling the NV centers to cavities/photonic band gap structures. Excellent progress has been made on all fronts. Ion implantation techniques seem ideally suited to the controlled creation of NV centres in diamond. The lift off technique has been shown to be capable of creating waveguides, mirrors and other optical structures. Preliminary data shows that it will be possible to Stark shift tune individual NV centres into resonance and provided that the required surface roughness can be attained, it should be possible to use a combination of lift-off and FIB techniques to create photonic band gap cavities in diamond. Finally, sophisticated, but entirely realizable primitives and architectures have been theoretically modeled that provide guidance to the sort of interesting structures and devices which can be fabricated in the near future.

Acknowledgments

The authors would like to thank Simon Devitt, and Ray Beasoleil for useful discussions in the preparation of this manuscript, and the Quantum Optics Group at HP Laboratories at Palo Alto for loan of diamond samples. This work was supported by the Australian Research Council, the Australian government and by the US National Security Agency (NSA), Advanced Research and Development Activity (ARDA) and the Army Research Office (ARO) under contracts W911NF-04-1-0290 and W911NF-05-1-0284.

References

[1] Blume-Kohout R, Caves CM and Deutsch IH 2002 *Found. Phys.* **32** 1641
[2] Davies EB 1977 *IEEE Transactions on Information Theory* **23** 530
[3] Belavkin VP 1983 *Autom. Remote Control (Engl. Transl.)* **44**, 178
[4] Wiseman HM and Milburn GJ 1993 *Phys. Rev. Lett.* **70**, 548
[5] Rabitz H, de Vivie-Riedle R, Motzkus M and Kompa K 2000, *Science* **288**, 824
[6] Bennett CH and Brassard G 1984 *Proc. IEEE Int. Conf. Computers, Systems and Signal Processing* 175
[7] Ekert AK 1991 *Phys. Rev. Lett.* **67**, 661
[8] Bennett CH, Brassard G, Crpeau C, Jozsa R, Peres A and Wootters WK 1993 *Phys. Rev. Lett.* **70**, 1895
[9] Huelga SF, Macchiavello C, Pellizzari T, Ekert AK, Plenio MB and Cirac JI 1997 *Phys. Rev. Lett.* **79**, 3865
[10] Boto AN, Kok P, Abrams DS, Braunstein SL, Williams CP and Dowling JP 2000 *Phys. Rev. Lett.* **85**, 2733
[11] Zaitsev AM 2001 *Optical Properties of Diamond: A Data Handbook*, (Berlin: Springer)
[12] Gruber A, Dräbenstedt A, Tietz C, Fleury L, Wrachtrup J and von Borczyskowski C 1997 *Science*, **276** 2012
[13] Beveratos A, Kühn S, Brouri R, Gacoin T, Poizat J-P and Grangier P 2002 *European Physical Journal D* **18**, 191
[14] Beveratos A, Brouri R, Gacoin T, Villing A, Poizat J-P and Grangier P 2002 *Phys. Rev. Lett.* **89**, 187901
[15] Jelezko F, Gaebel T, Popa I, Gruber A and Wrachtrup J 2004 *Phys. Rev. Lett.* **92**, 076401
[16] Howard M, Twamley J, Wittmann C, Gaebel T, Jelezko F and Wrachtrup J 2005 Quantum process tomography of a single solid state qubit *Preprint* quant-ph/0503153
[17] Greentree AD, Wei C, Holmstrom SA, Martin JPD, Manson NB, Catchpole KR and Savage C 1999 *J. Opt. B: Quantum Semiclass. Opt.* **1**, 240
[18] Wei C, Holmstrom SA, Greentree AD and Manson NB 1999 *J. Opt. B: Quantum Semiclass. Opt.* **1**, 289
[19] Greentree AD, Wei C and Manson NB 1999 *Phys. Rev. A* **59**, 4083
[20] Wei C and Manson NB 1999 *J. Opt. B: Quantum Semiclass. Opt.* **1**, 464
[21] Wilson EA, Manson NB and Wei C 2003 *Phys. Rev. A* **67**, 023812
[22] Jelezko F, Gaebel T, Popa I, Domhan M, Gruber A and Wrachtrup J 2004 *Phys. Rev. Lett.* **93**, 130501
[23] ARDA Roadmap, `http://qist.lanl.gov`, (2004).
[24] Rabeau JR, S. T. Huntington ST, Greentree AD and Prawer S 2005 *Appl. Phys. Lett.* **86**, 134104
[25] Parikh NR, Hunn JD, McGucken E, Swanson ML, White CW, Rudder RA, Malta DP, Posthill JB and Markunas R 1992 *Appl. Phys. Lett.* **61**, 3124
[26] Olivero P, Rubanov S, Reichart P, Gibson BC, Huntington ST, Rabeau JR, Greentree AD, Salzman J, Moore D, Jamieson DN and Prawer S 2005 *Advanced Materials* **17**, 2427
[27] Jamieson DN, Yang C, Hopf T, Hearne SM, Pakes CI, Prawer S, Mitic M, Gauja E, Andresen SE, Hudson FE, Dzurak AS and Clark RG 2005 *Appl. Phys. Lett.* **86**, 202101
[28] Meijer J, Burchard B, Domhan M, Wittmann C, Gaebel T, Popa I, Jelezko F and Wrachtrup J 2005 Generation of single colour centers by focussed nitrogen implantation *Preprint* cond-mat/0505063
[29] DiVincenzo DP 1995 *Phys. Rev. A* **51**, 1015
[30] Chuang IL, Vandersypen LMK, Zhou X, Lueng DW and Lloyd S 1998 *Nature (London)* **393** 143

[31] Turchette QA, Hood CJ, Lange W, Mabuchi H and Kimble HJ 1995 *Phys. Rev. Lett.* **75**, 4710
[32] Cirac JI, Zoller P, Kimble HJ and Mabuchi H 1997 *Phys. Rev. Lett.* **78**, 3221
[33] Lovett BW, Reina JH, Nazir A and Briggs GAD 2003 *Phys. Rev. B* **68**, 205319
[34] Knill E, Laflamme L and Milburn GJ 2001 *Nature (London)* **409**, 46
[35] Childress LI, Taylor JM, Sørensen AS and Lukin MD 2005 Fault-tolerant quantum repeaters with minimal physical resources, and implementations based on single photon emitters *Preprint* quant-ph/0502112
[36] Greentree AD, Salzman J, Prawer S and Hollenberg LCL 2005 Quantum gate for Q switching in monolithic photonic bandgap cavities containing two-level atoms *Preprint* quant-ph/0511107
[37] Brewer RG and Shoemaker RL 1971 *Phys. Rev. Lett.* **27** 631
[38] Collins AT, Thomaz MF and Jorge MIB 1983 *J. Phys. C: Solid State Phys.* **16**, 2177
[39] Kaplyans AA, Kolyshki VI and Medvedev VN 1970 *Soviety Physics Solid State* **12** 1193
[40] Davies G and Manson NB 1980 *Industrial Diamond Review* **50** 1980
[41] Redman D, Brown S and Rand SC 1992 *J. Opt. Soc. Am. B* **9**, 768
[42] Geis MW, Efremow NN and Rathman DD 1988 *Journal of Vacuum Science and Technology A: Vacuum, Surfaces, and Films* **6**, 1953
[43] Lukin MD and Hemmer PR 2000 *Phys. Rev. Lett.* **84**, 2818
[44] Shahriar MS, Hemmer PR, Lloyd S, Bhatia PS and Craig AE 2002 *Phys. Rev. A* **66** 032301
[45] Milburn GJ 1989 *Phys. Rev. Lett.* **62** 2124
[46] Chuang IL and Yamamoto Y 1995 *Phys. Rev. A* **52**, 3489
[47] Gerry CC 1999 *Phys. Rev. A* **59**, 4095
[48] Harris SE, Field JE and Imamoğlu A 1990 *Phys. Rev. Lett.* **64**, 1107
[49] Munro WJ, Nemoto K, Beausoleil RG and Spiller TP 2005 *Phys. Rev. A* **71**, 033819
[50] Munro WJ, Nemoto K, Spiller TP, Barrett SD, Kok P and Beausoleil RG 2005 *J. Opt. B: Quantum Semiclass. Opt.* **7**, S135
[51] Nemoto K and Munro W 2005 *Phys. Rev. Lett.* **93**, 250502
[52] Spiller TP, Nemoto K, Braunstein SL, Munro WJ, van Loock P, and Milburn GJ 2005 Quantum Computation by Communication *Preprint* quant-ph/0509202
[53] Munro WJ, Private communications
[54] Charnock FT and Kennedy TA 2001 *Phys. Rev. B* **64**, 041201(R)
[55] Kennedy TA, Charnock FT, Colton JS, Butler JE, Linares RC and Doering PJ 2002 *Phys. Status Solidi* **233**, 416
[56] Kennedy TA, Colton JS, Butler JE Linares RC and Doering PL 2003 *Appl. Phys. Lett.* **83**, 4190
[57] Gaebel T *et al in preparation*
[58] Lim YL, Beige A and Kwek LC 2005 *Phys. Rev. Lett.* **95**, 030505
[59] Barrett SD and Kok P 2005 *Phys. Rev. A* **71**, 060310(R)
[60] Benjamin SC, Eisert J and Stace TM 2005 *New J. Phys.* **7**, 194
[61] Lim YL, Barrett SD, Beige A, Kok P and Kwek LC 2005 Repeat-Until-Success quantum computing using stationary and flying qubits *Preprint* quant-ph/0508218
[62] Nielsen MA and Chuang IL 2000 *Quantum computation and quantum information* (Cambridge University Press)
[63] Devitt SJ, Greentree AD and Hollenberg LCL 2005 Information free quantum bus for universal quantum computation *Preprint* quant-ph/0511084
[64] Raussendorf R and Briegel HJ 2001 *Phys. Rev. Lett.* **86**, 5188
[65] Nielsen MA 2004 *Phys. Rev. Lett.* **93**, 040503
[66] Browne DE and Rudolph T 2005 *Phys. Rev. Lett.* **95**, 010501
[67] Walther P, Resch KJ, Rudolph T, Schenck E, Weinfurter H, Vedral V, Aspelmeyer M and Zeilinger A 2005 *Nature (London)* **434**, 169
[68] Benjamin SC, Browne DE, Fitzsimons J and Morton JJL 2005 Brokered Graph State Quantum Computing *Preprint* quant-ph/0509209
[69] Björman H, Rangsten P and Hjort K 1999 *Sensors and Actuators* **78**, 41
[70] Fu Y and Du HJ 2001 *Proc. SPIE* **4557**, 24
[71] Ramanathan D and Molian PA 2002 *Journal of Manufacturing Science and Engineering* **124**, 389
[72] Hunn JD and Christensen CP 1994 *Solid State Technol.* **37**,57
[73] Sekaric L, Parpia JM, Craighead HG, Feygelson T, Houston BH and Butler JE 2002 *Appl. Phys. Lett.* **81**, 4455
[74] Auciello O, Birrell J, Carlisle JA, Gerbi JE, Xiao X, Peng B and Espinosa HD 2004 *J. Phys.: Condens. Matter* **16**, R539
[75] Hunn JD, Withrow SP, White CW, Clausing RE, Heatherly L, Christensen CP and Parikh NR 1995 *Nucl. Instr. and Meth. in Phys. Res. B* **99**, 602

[76] Prawer S 1995 *Diamond Related Materials* **4** 862
[77] Prawer S and Kalish R 1995 *Phys. Rev. B* **51** 15711
[78] Orwa JO, Nugent KW, Jamieson DN and Prawer S 2000 *Phys. Rev. B* **62** 5461
[79] Breese MBH, Jamieson DN and King PJC 1996, in *Material Analysis Using a Nuclear Microprobe*, (John Wiley and Sons Inc., New York)
[80] Ramanathan D and Molian PA 2002 *J. Manufacturing Sci. Eng.Trans. ASME* **124**, 389
[81] Karlsson M and Nikolajeff 2003 *Optics Express* **11**, 502
[82] Fu Y and Bryan NKA 2003 *Opt. Eng.* **42**, 2214
[83] Marchywka M, Pehrsson PE, Binari SC and Moses D 1993 *J. Electrochemical Soc.* **140**, L19
[84] Adams DP, Vasile MJ, Mayer TM and VC Hodges 2003 *J. Vac. Sci. Technol. B* **21**, 2334
[85] Olivero P, Rubanov S, Reichart P, Gibson BC, Huntington ST, Rabeau JR, Greentree AD, Salzman J, Moore D, Jamieson DN and Prawer S 2005 *Diam. Rel. Mater.* submitted for publication
[86] Nishida Y, Mita Y, Mori K, Okuda S, Sato S, Yazu S, Nakagawa M and Okada M 1989 *Materials Sci. Forum* **38-41**, 561
[87] Mita Y 1996 *Phys. Rev. B* **53**, 11360
[88] Martin J, Wannemacher R, Teichert J, Bischoff L and Köhler B 1999 *Appl. Phys. Lett.* **75**, 3096
[89] Kalish R, Uzan-Saguy C, Philosoph B, Richter V, Lagrange JP, Gheeraert E, Deneuville A, Collins AT 1997 *Diamond and Related Materials* **6** 516
[90] Ziegler JF, Biersack JP and Littmark U 1985 *The Stopping and Range of Ions in Solids* (Pergamon, New York)
[91] Rabeau JR, Reichart P, Tamanyan G, Jamieson DN, Prawer S, Jelezko F, Gaebel T, Popa I, Domhan M, Wrachtrup J 2005 Implantation of labelled single nitrogen vacancy centers in diamond using ^{15}N *Preprint* cond-mat/0511722
[92] Tarutani M, Shimato Y, Takai Y and Shimizu R 1995 *Appl. Phys. Lett.*, **67**, 632
[93] Nugent KW and Prawer S 1998 *Diamond and Related Materials*, **7**, 215
[94] Prins JF 1988 *Phys. Rev. B* **38**, 5576